Proceedings of the International Conference
on Computational and Mathematical Methods
in Science and Engineering, CMMSE 2009
30 June, 1–3 July 2009.

Geometric greedy and greedy points for RBF interpolation

Stefano De Marchi[1]

[1] *Department of Computer Science,, University of Verona, Italy*

emails: `stefano.demarchi@univr.it`

Abstract

In this note we present some quantitative results concerning the convergence proofs of the *Greedy Algorithm* and the *Geometric Greedy Algorithm*, presented in [4], for finding near-optimal points for radial basis functions interpolation.

Key words: Greedy algorithm, radial basis functions, kernel methods.

1 Introduction

In [4] the authors constructed a data-independent near-optimal points set for interpolation by radial basis functions (RBF). In that paper, there were also presented two different *greedy algorithms* for computing near-optimal points for RBF interpolation.

For the sake of completeness, here we briefly recall some notations and results from [4] useful to understand the rest of the paper.

Let $\Omega \subset \mathbb{R}^d$ be a bounded subset of $\mathbb{R}^d$ satisfying a inner cone condition with angle α and radius r.

The first algorithm, termed *Greedy Algorithm*, shortly G.A., generates larger and larger point sets, say $X_n = \{x_0, \ldots, x_{n-1}\} \subset \Omega$, by adding at each step a new point corresponding to the point where the *power function*, $P_{\Phi,X_{n-1}}$, of the previous set attains its maximum. In practice, starting from the set $X_0 = \{x_0\}$, $x_0 \in \Omega$ arbitrarily chosen, the method constructs $X_n = X_{n-1} \cup \{x_n\}$ where

$$P_{\Phi,X_{n-1}}(x_n) = \|P_{\Phi,X_{n-1}}\|_{L_\infty(\Omega)}, \;\forall\, n \geq 1. \tag{1}$$

Practical experiments showed that the greedy approach fills the current largest hole in the data, placing the new point nearby the center of the hole.

This observation, suggested to investigate a second algorithm, that we called *Geometric Greedy Algorithm*, shortly G.G.A., that was shown to be *independent* on the kernel Φ. Indeed, the method starts from $X_0 = \emptyset$ and, at the nth step produces the finite set X_n, of cardinality n, where $X_n = X_{n-1} \cup \{x_n\}$ and

$$x_n = \max_{x \in \Omega \setminus X_{n-1}} d(x, \Omega)\,. \tag{2}$$

The distance d in (2), was the L_2 norm. It was also observed (cf. [4, Lemma 5.1]) that the G.G.A. generates point sets that are asymptotically equidistributed with respect to the distance d.

Later, in the paper [3] it was shown that, given a metric ν, sequences of points generated by means of the G.G.A. are asymptotically equidistributed in the compact set Ω with respect to the given metric ν. Moreover, it was noticed that the construction technique of the geometric greedy algorithm is conceptually similar to that used in producing univariate *Leja sequences* (cf. [2]). The reason relies on that fact that both in the case of Leja sequences and in (2), one maximizes a function of distances from already computed points (taken from a suitable discretization of Ω).

For the G.G.A. we already proved (cf. [4, Lemma 5.1]) that the points generated are equidistributed in the L_2-norm and that h_n behaves asymptotically like $\mathcal{O}(n^{-1/d})$.

In this paper, we would like to provide more numerical evidence of the fact that the G.G.A. generates sequences of points which are equidistributed in Ω with respect to the L_2-norm and whose separation distances, h_n, behaves asymptotically also like $\mathcal{O}(n^{-1/d})$. A quantitative analysis of the constants involved in this asymptotic analysis is studied, too. Concerning the G.A., we shall notice that

2 Results

Let $\Omega \subset \mathbb{R}^d$ be a bounded subset of $\mathbb{R}^d$ satisfying a inner cone condition with angle α and radius r. Letting $X_n = \{x_1, \ldots, x_n\} \subset \Omega$ and $h_n = \sup_{y \in \Omega} \min_{x \in X_n} \|x - y\|_2$, $q_n = \frac{1}{2} \min_{\substack{x,y \in X_n \\ x \neq y}} \|x - y\|_2$ as usual the *fill distance* and the *separation distance*, and $B_r(x) = \{y \in \mathbb{R}^d : \|x - y\|_2 < r\}$.

2.1 The G.G.A. case

First of we recall an interesting result proved for set of points quasi-uniformly distributed, which means that $\exists M_1, M_2 \in \mathbb{R}_+$ such that $M_1 \leq \frac{h_n}{q_n} \leq M_2$, $\forall n \in \mathbb{N}$ (cf. [8, Prop. 14.1]).

Proposition 2.1 *There exists constants* c_1 , $c_2 \in \mathbb{R}$, $n_0 \in \mathbb{N}$ *such that*

$$c_1\, n^{-1/d} \leq h_n \leq C_2\, n^{-1/d}, \quad \forall n \geq n_0.$$

Proof: Taking the n balls $B_{q_n}(x_j)$, than always

$$n\, q_n^d \mathrm{vol}(B_1) \leq \mathrm{vol}(\Omega)\,, \tag{3}$$

where B_1 is the unit ball of $\mathbb{R}^d$, from which the upper bound follows from the assumption that $h_n \le M_2\, q_n$. For the lower bound, one observes that $\Omega \subseteq \bigcup_{i=1}^n B_{h_n}(x_j)$, hence

$$\mathrm{vol}(\Omega) \le n\, h_n^d \frac{\sqrt{\pi^d}}{\Gamma(d/2+1)} \tag{4}$$

from which the lower bound follows. □

In many applications one requires a quantitative value to the constants involved, especially for the upper bound. Here some computations showing that the constants depend on the volume of the set Ω and the upper bound, M_2 for the ratio h_n/q_n

$$\begin{aligned}
\mathrm{vol}(\Omega) &\ge \mathrm{vol}\left(\Omega \cap \bigcup_{j=1}^n B_{x_j}(q_n)\right) = \sum_{j=1}^n \mathrm{vol}\left(\Omega \cap B_{x_j}(q_n)\right)\\
&\ge \frac{\alpha}{2\pi}\sum_{j=1}^n \min\{\mathrm{vol}\left(B_0(q_n)\right), \mathrm{vol}\left(B_0(r)\right)\}\\
&= n\frac{\alpha}{2\pi}\frac{\pi^{d/2}}{\Gamma(d/2+1)}\min\{(q_n)^d, r^d\}
\end{aligned}$$

But r does not depend on n and $\mathrm{vol}(\Omega)$ is fixed, therefore there must be a $n_0 \in \mathbb{N}$ with

$$\mathrm{vol}(\Omega) \ge n\frac{\alpha}{2\pi}\frac{\pi^{d/2}}{\Gamma(d/2+1)}(q_n/2)^d, \quad \forall n \ge n_0.$$

Defining C_Ω by

$$C_\Omega := \frac{\mathrm{vol}(\Omega)2^{d+1}\pi\Gamma(d/2+1)}{\alpha\pi^{d/2}}, \tag{5}$$

we get

$$C_\Omega \ge n(q_n)^d \ge n(h_n/M_2)^d.$$

Hence,

$$h_n \le M_2(C_\Omega/n)^{1/d} = \underbrace{C_\Omega^{1/d}M_2}_{=:C_{\Omega,M_2}} n^{-1/d}\ . \tag{6}$$

In the next session, we present some numerical experiments that support the theoretical results just provided.

2.1.1 Numerical experiments for the G.G.A.

Let $\Omega = [-1,1]^2$, so that $d = 2$. For our experiments we considered five sets of points

1. *Leja-like points* generated by using the G.G.A. by means of the formula (2) and L_2 norm, obtained by discretizing Ω by 10^4 random points. For this set we computed 406 points, that we consider here for our experiments.

2. Points generated by using the G.A. (cf. formula (1)), obtained as described in [4]: 134 points for the inverse multiquadrics and 200 points for the Wendland $\mathcal{C}^2$ function. In both case the scaling factor was taken equal to 1, the threshold was set to $1.0e-6$ for the inverse multiquadrics and $1.0e-3$ for the Wendland function. The domain Ω were discretized with a 300×300 grid.

3. *Dubiner points* in the square, i.e. points equally distributed in the Dubiner metric in the unit square (cf. [3]). For this set we considered 200 points.

4. *P-greedy points.* These points were obtained by S. Müller [6], for two positive definite kernels, the gaussian and the $\mathcal{C}^{\in}$ Wendland's kernel, by discretizing Ω by a grid of 300×300 points, taking the scaling parameter equal to 1 (i.e. no scaling). We observe that these points, correspond essentially to the ones computed by the G.A.. They are slightly different due to a different stopping test used during computations. For this set we considered 300 points computed using the Wendland's kernel with shape parameter set to 1, i.e. without scaling.

In Figures 1-5, for all the set of points, we show at the left, the plots of the uniformity h_n/q_n while, at the right, the plots of $h_n/C_{\Omega,M}$ versus $1/\sqrt{n}$. In Figures 6-10 we show the plots of h_n versus $C_{\Omega,M}$.

A close inspection to these graphs suggests some observations.

1. In almost all graphs, varying n, $h_n < C_{\Omega,M}$, which says that a better upper bound should be derived.

2. From (6), $h_n/C_{\Omega,M}$ should be bounded by $1/\sqrt{n}$. For the set of Leja-like points we see that $h_n/C_{\Omega,M} \le n^{-1/2}$ for all n. This comes evident in Figures 1-5 (Left part) where the *uniformity* h_n/q_n of the sets of test points is plotted. In all cases the uniformity is bounded, especially for bigger n. The reason why the inequality (6) holds only for the Leja-like points, is due to the fact that in the computations we chose $C_\Omega = n\,q_n^d$ while it should be $C_\Omega \ge n\,q_n^d$. Therefore, taking bigger values for the constants C_Ω then the ratio $h_n/C_{\Omega,M}$ will become smaller moving the graphs below. That is to say, that the choice $C_\Omega = n\,q_n^d$ does not hold for all sets of equidistributed points.

In Table 1 we also report the values of $\max(C_{\Omega,M})$ and $\min(C_{\Omega,M})$ compared with the corresponding values of $\max(h_n)$, $\min(h_n)$ and $\max(q_n)$, $\min(q_n)$.

2.2 The G.A. case

More intriguing is the case of greedy points generated by the G.A.. In [5], the authors have introduced the concept of *best-packing configurations* for an infinite set $A \subset \mathbb{R}^d$. For a set $X_n = \{x_1, \dots, x_n\} \subset \mathbb{R}^d$ of n points we consider

$$\delta(X_n) = \min_{i \neq j} \|x_i - x_j\|_2 \,,$$

	406 Leja-like pts.	134 IM pts.	200 W2 pts.	200 Dubiner pts.	300 P-greedy pts.
$\max(C_{\Omega,M})$	8.99	8.14	7.92	5.95	6.93
$\min(C_{\Omega,M})$	1	0.315	1	0.072	1
$\max(h_n)$	1.99	1.42	1.42	2.08	2.01
$\min(h_n)$	0	0.085	0.009	0	0.003
$\max(q_n)$	1	1	1	1	1
$\min(q_n)$	0.09	0.05	0.11	0.02	0.06

Table 1: A comparison of $\max(C_{\Omega,M})$ and $\max(h_n)$, $\min(C_{\Omega,M})$ and $\min(h_n)$for the five different types of point distributions.

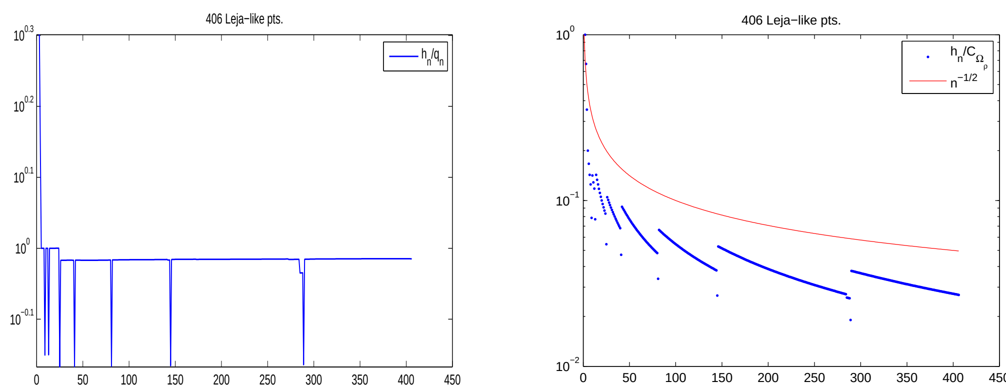

Figure 1: Left: the plots of the uniformity h_n/q_n for 406 Leja-like points. Right: plots of $h_n/C_{\Omega,M}$ and $1/\sqrt{n}$.

while for an infinite set, we let $A \subset \mathbb{R}^d$

$$\delta_n(A) = \sup\{\delta(X_n) \ : \ X_n \subset A, \mathrm{card}(X_n) = n\}$$

be the *best-packing distance*. This distance is simply the *fill distance* in RBF setting. Moreover, the authors define the idea of *greedy best-packing configuration* on an infinite compact subset $A \subset \mathbb{R}^d$ in the following way:

- select arbitrarily the initial point $a_0 \in A$;
- at the step n, $a_n \in A$ is chosen as

$$\min_{0 \le i \le n-1} \|a_n - a_i\|_2 = \max_{x \in A} \min_{0 \le i \le n-1} \|x - a_i\|_2 \, . \tag{7}$$

Such points were already considered in [2] where it was proposed the name *Leja-Bos points* (thanks to L. Bos who suggested the definition (7)).

In [5, Prop. 2.13], it has been proved that in the square $[0,1]^2$ there exists greedy best-packing configurations which are not asymptotically uniformly distributed, and the Leja-Bos points are an example.

The constructive proof checks the best-packing property by using the Voronoi cell decomposition associated to the points. In particular, they showed that Leja-Bos points *are not* asymptotically uniformly distributed since the subsequence consisting of $N(n) = 3 \cdot 2^{2(n-1)} + 7 \cdot 2^{n-2} + 1$ points, holds

$$\lim_{n\to\infty} \frac{\mathrm{card}(T_{N(n)} \cap [0,1/2] \times [0,1])}{N(n)} = \lim_{n\to\infty} \frac{(2^{n-1}+1)(2^n+1)}{N(n)} = \frac{2}{3} \neq \frac{1}{2}\,, \tag{8}$$

where $T_{N(n)}$ indicates the subsequence of Leja-Bos points consisting of $N(n)$ points (for more details cf. [5, Proof of Prop. 2.13]).

2.2.1 Numerical experiments for the G.A.

On the basis of the above considerations, it seems *natural* that a simple direction of investigation, for checking if the points generated by the G.A. are asymptotically distributed w.r.t. the L_2 metric, is to verify if they form a greedy best-packing set and how far are from the Leja-Bos points.

So far, we have not any theoretical results but only numerical experiments. To this aim, we computed the *root mean square error*, RMSE, of the fill-distances between the Leja-Bos points (the best-packing set) and the set of points, considered in the previous session §2.1.1. What is immediately visible is that, for almost all point sets computed by the G.A. they distribute as Leja-Bos points. Indeed, all errors in Table 2 are decreasing at the number of points increases, independently of the kernel used for their computation. The worse error, as expected, is obtained for the Dubiner points (in bold) which are not related to any radial kernel.

	134 IM pts.	200 W2 pts.	200 Dubiner pts.	300 P-greedy pts.	406 Leja-like pts.
RMSE	0.0775	0.0773	**0.1270**	0.0543	0.0233

Table 2: A comparison of the root mean square errors, between the fill-distances of Leja-Bos points and the set of points already considered in §2.1.1.

For completeness, in Figures 11 and 12, we show 406 Leja-Bos points, the Voronoi tiles associated to the Leja-Bos points and their mutual fill-distances.

2.2.2 Remarks

1. Except for the Dubiner points, the greedy points computed by the G.A. behave as the greedy best-packing points. It seems reasonable to prove that they could not be uniformly equidistributed in the L_2 norm.

2. In all experiments we noticed that the fill distances between Leja-Bos points and the corresponding points considered in §2.1.1, behave almost similarly. For the case of 406 Leja-Bos and Leja-like points see Figure 12.

3. It is worth mention that the problem of finding well-distributed points depending on the kernel, can be viewed as a special instance of the more general *disk covering*

problem that, in 2 and 3-dimensions, are known as disks and spheres packing, respectively (cf. e.g. in [1, 9]). Therefore, in 2d and 3d, we have two possibilities to check if the points generated by the greedy algorithm are optimal:

(a) form a greedy best-packing configuration;

(b) solve a disk or sphere packing problem.

Acknowledgements

This work has been supported by ex 60% funds of the University of Verona.

References

[1] Boll, D.W., Donovan, J, Graham, R. L. and Lubachevsky, B. D. *Improving Dense Packings of Equal Disks in a Square*, Elect. J. Combinatorics, Vol. 7 (2000), R 46.

[2] De Marchi, S. *On Leja sequences: some results and applications*, Appl. Math. Comput., Vol. 152(3) (2004), 621-647.

[3] Caliari, M., De Marchi, S., and Vianello, M. *Bivariate polynomial interpolation on the square at new nodal sets*, Appl. Math. Comput., Vol. 165(2) (2005), 261-274.

[4] De Marchi, S., Schaback, R. and Wendland, H. *Near-Optimal Data-independent Point Locations for Radial Basis Function Interpolation*, Adv. Comput. Math., Vol. 23(3) (2005), 317-330.

[5] López García, A. and Saff, E. B. *Asymptotics of greedy energy points*, available at the web page of the second author.

[6] Müller, S. Matlab files in [7].

[7] Müller, S. and Schaback, R. *Newton Basis for Kernel Spaces*, J. Approx. Theory, Available online 10 December 2008, doi:10.1016/j.jat.2008.10.014.

[8] Wendland, H. Scattered Data Approximation, Cambridge Univ. Press, 2005.

[9] Weisstein, Eric W. *Circle Packing.* From MathWorld–A Wolfram Web Resource. http://mathworld.wolfram.com/CirclePacking.html

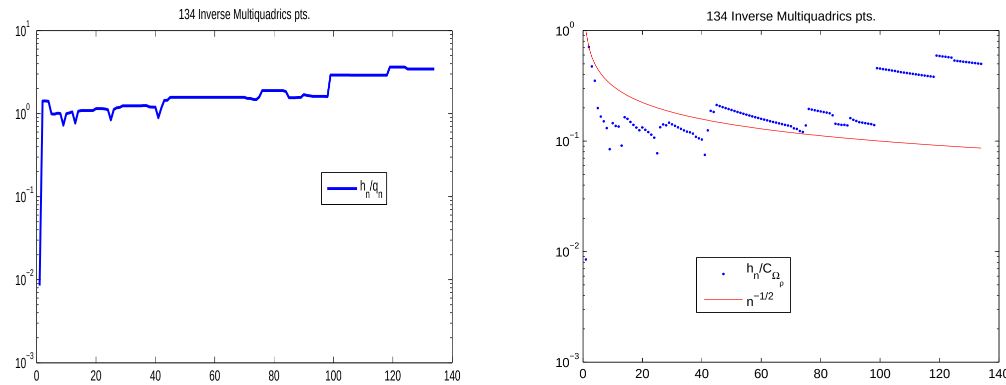

Figure 2: Left: the plots of the uniformity h_n/q_n for 134 points for the inverse multiquadrics. Right: plots of $h_n/C_{\Omega,M}$ and $1/\sqrt{n}$.

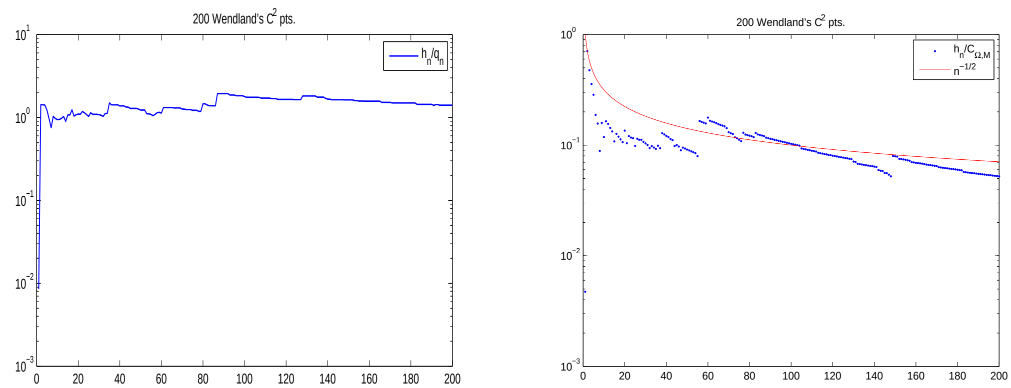

Figure 3: Left: the plots of the uniformity h_n/q_n for 200 points for the Wendland's function. Right: plots of $h_n/C_{\Omega,M}$ and $1/\sqrt{n}$.

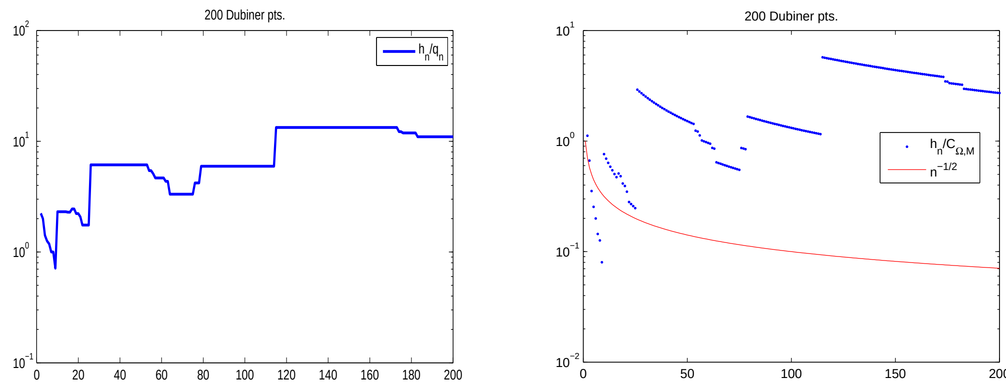

Figure 4: Left: the plots of the uniformity h_n/q_n for 200 Dubiner points. Right: plots of $h_n/C_{\Omega,M}$ and $1/\sqrt{n}$.

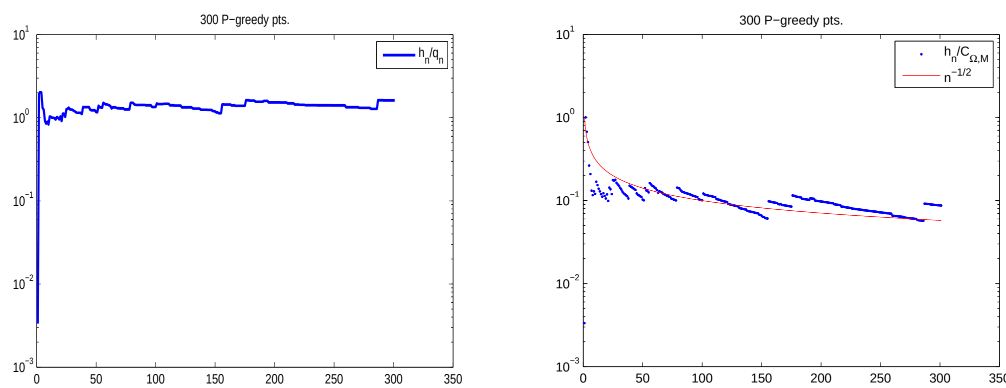

Figure 5: Left: the plots of the uniformity h_n/q_n for 300 P-greedy points. Right: plots of $h_n/C_{\Omega,M}$ and $1/\sqrt{n}$.

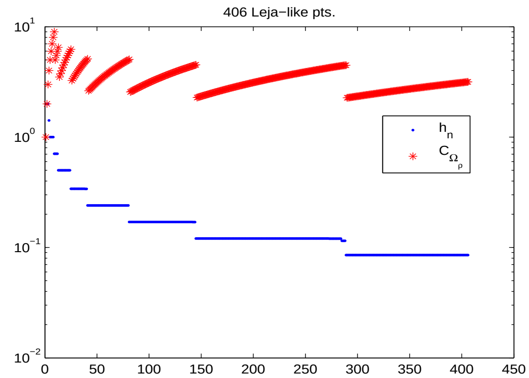

Figure 6: The plots of h_n and $C_{\Omega,M}$ for 406 Leja-like points.

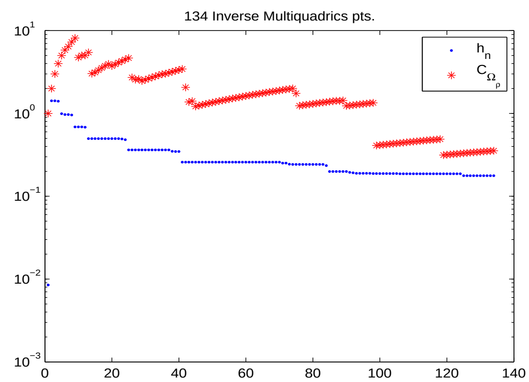

Figure 7: The plots of h_n and $C_{\Omega,M}$ for 134 inverse multiquadrics points.

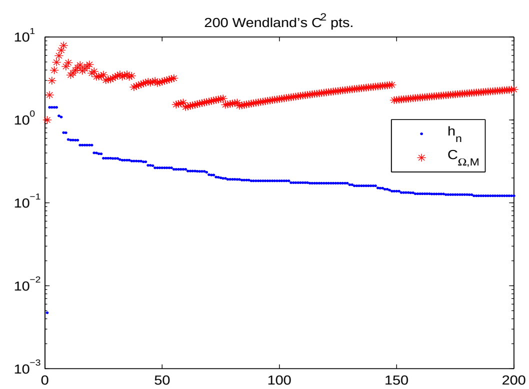

Figure 8: The plots of h_n and $C_{\Omega,M}$ for 200 Wendland $\mathcal{C}^2$ points.

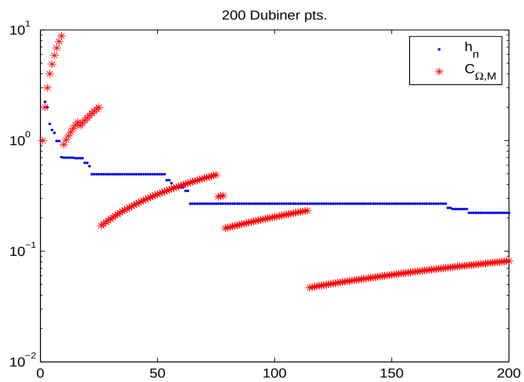

Figure 9: The plots of h_n and $C_{\Omega,M}$ for 200 Dubiner points.

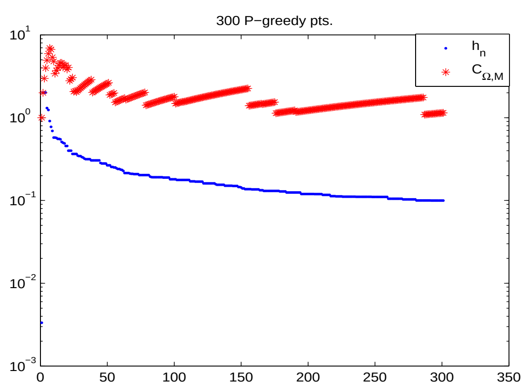

Figure 10: The plots of h_n and $C_{\Omega,M}$ for 300 P-greedy points.

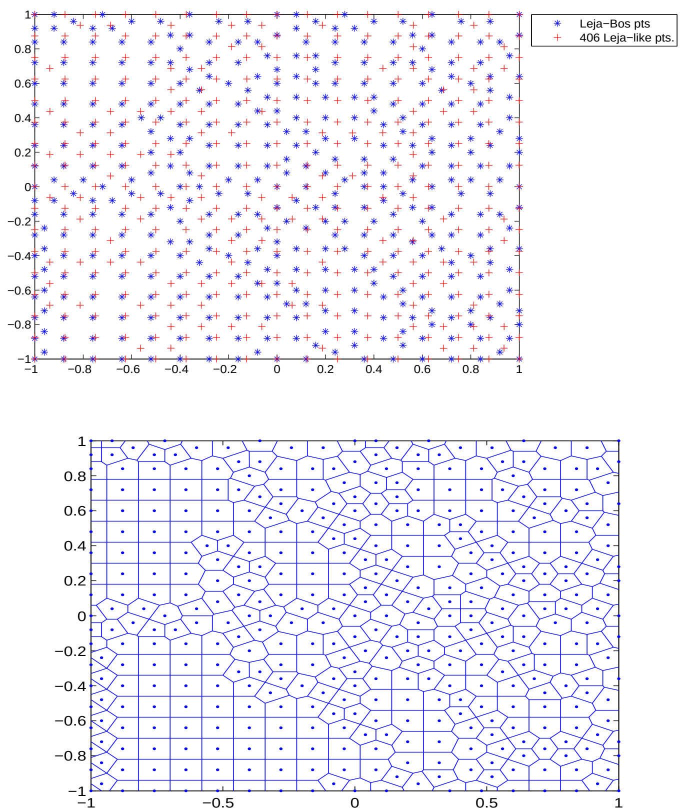

Figure 11: 406 Leja-Bos and Leja-like points (above). The Voronoi tiles for the 406 Leja-Bos points (below)

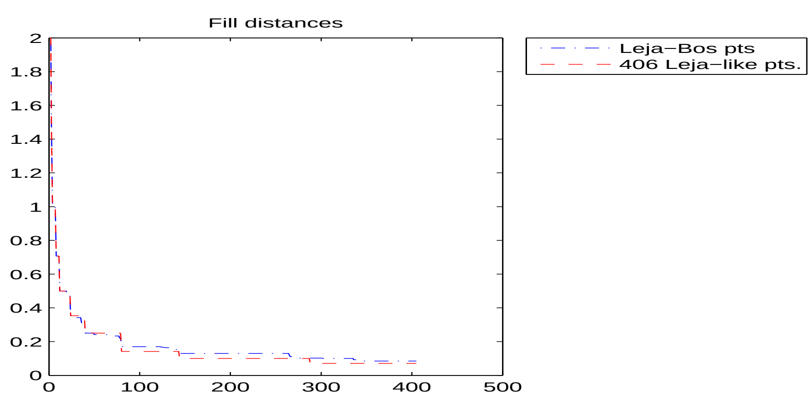

Figure 12: The plots of the fill-distances for 406 Leja-Bos and Leja-like points